Mathematical model for positive feedback and temperature induced signal transduction and differential gene regulation in *Bordetella pertussis*

Arnab Bandyopadhyay[1, a)] and Suman K Banik[1, b)]
Department of Chemistry, Bose Institute, 93/1 A P C Road, Kolkata 700 009, India

(Dated: 3 June 2011)

Based on the phosphorelay kinetics operative within BvgAS two component system we propose a mathematical model for signal transduction and differential gene regulation in *Bordetella pertussis*. To understand the system behavior under elevated temperature, the developed model has been studied in two different ways. First, a quasi-steady state analysis has been carried out for the two component system, comprising of sensor BvgS and response regulator BvgA. The quasi-steady state analysis reveals a positive feedback and temperature induced molecular switch, leading to graded response and amplification in the output of BvgA. Accumulation of large pool of BvgA thus results into differential regulation of the downstream genes, including the gene encoding toxin. Furthermore, numerical integration of the full network kinetics has been carried out to explore time dependent behavior of different system components, that qualitatively capture the essential features of experimental results performed *in vivo*.

PACS numbers: 82.39.-k, 87.16.Xa, 87.18.Mp, 87.18.Vf

I. INTRODUCTION

One of the important functional aspects of living organisms is to respond to the sudden changes made in their environment, and to make appropriate changes in the cellular or subcellular level for survival. Direct manifestations of such changes at the subcellular level are the expression/repression of single or multiple genes controlling different functional behavior of an organism.[1] The human pathogen *Bordetella pertussis*, a gram negative bacteria and causative agent for the disease whooping cough,[2] is no exception to the aforesaid behavior. At 25 °C, while freely moving in the environment their pathogenic properties remain dormant. But, when they are within the host at 37 °C, their virulent properties come into play. In the laboratory the reverse effect, i.e., suppression of pathogenic behavior is observed using $MgSO_4$ or nicotinic acid.[3,4] The virulent behavior of *B. pertussis* within host, in response to sudden environmental change, has been experimentally studied and has been found to be operative through BvgAS two component system (TCS).[3,4] The TCS comprises of transmembrane sensor BvgS and response regulator BvgA where signal flows through this pair via a four step (His-Asp-His-Asp) phosphorelay mechanism.

As a response to temperature elevation in the environment, the response regulator BvgA becomes active (the phosphorylated dimer) within each bacterium, which in turn exerts a positive feedback on its own operon, the *bvg* operon. Positive feedback loop thus increases the active form of BvgA in a switch like manner. In other words, once the BvgAS two-component machinery becomes operative, large pool of active BvgA either repress and/or express several downstream genes where the phosphorylated dimer of BvgA plays the leading role by acting as transcription factor (TF).[5] Based on the binding affinity of TFs to the respective promoters, different types of downstream genes are regulated in *Bordetella spp.* and have been broadly grouped into four classes, e.g., class 1, class 2, class 3 and class 4.[3,4] Class 1 genes encompass genes that are responsible for encoding toxins, such as adenylate cyclase (*cyaA-E*) and pertussis toxin (*ptxA-E*). Class 2 genes express proteins responsible for adherence, such as *fhaB* encodes filamentous hemagglutinin. Among all the four classes of genes, class 3 genes show a unique behavior, although its functional activity is not known till date.[3,4] The only well characterized class 3 gene found in *B. pertussis* is known as *bipA*. The final one, class 4 genes have been reported to encode *frlAB* in *B. bronchiseptica* and is responsible for motility. It is important to mention that expressions of class 3 and class 4 gene are not observed in *B. pertussis* under the influence of temperature elevation. To be specific, class 3 gene expression has been observed in *B. pertussis* only under the influence of intermediate concentration of $MgSO_4$ and class 4 gene under low concentration of $MgSO_4$ in *B. bronchiseptica*. Expression and/or repression of the four classes of downstream genes is controlled by strong and/or weak binding sites (for TFs) present in the promoter region of the respective genes. Among these, promoter region of class 4 gene has the strongest affinity for TFs. Promoter region of class 2 and class 3 genes have medium affinity for TFs, whereas promoter region of class 1 gene has the weakest affinity for TFs. On the basis of the promoter regions' affinity for TFs it is thus expected that expression and/or repression of four classes of downstream genes in *Bordetella spp.* would show a differential pattern in their temporal dynamics.

[a)] Electronic mail: arnabbanerjy@gmail.com
[b)] Electronic mail: skbanik@bic.boseinst.ernet.in; Corresponding author

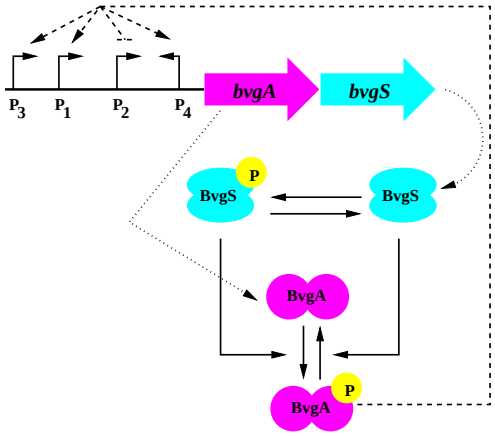

FIG. 1. (color online) Schematic presentation of *bvg* locus and signal transduction in BvgAS two component system. The dashed line presents the feedback by phosphorylated dimer of BvgA on its own operon. The dotted line is for the production of dimers of BvgS and BvgA. For simplicity the mRNAs are not shown in the diagram.

Keeping these aforesaid phenomenological information in mind we have developed a mathematical model based on biochemical interactions taking place within *B. pertussis* under the influence of temperature elevation. The objective of present work is twofold. First, we aim to understand the molecular switch operative in BvgAS TCS and to identify the key players responsible for amplification of TFs. Second, through our model we aim to regenerate qualitative features of the network and to mimic different phenotypic states of *B. pertussis* under temperature elevation.

The paper is organized in the following way. In the next section we describe the mathematical model using possible key biochemical kinetic interactions. In section 3, we first provide a steady state analysis of the TCS and then extend our analysis via computer simulation of the full network kinetics, where qualitative features of the *in vivo* experimental results have been presented. The paper is concluded in section 4.

II. THE MODEL

To understand the mechanism for temperature induced activation of *bvg* locus and differential regulation of the downstream genes, we propose a mathematical model in the following.

A. The bvg locus

Experimental studies in *B. pertussis* suggest multi-promoter activities in *bvg* operon.[6–8] Out of the four promoters, P_1, P_2, P_3 and P_4, present in the *bvg* locus (see Fig. 1), only P_2 is known to be constitutively active under non-inducing condition (25 °C) and is *bvg* independent. After induction (37 °C), activity of the P_2 promoter goes down while the other three promoters (P_1, P_3 and P_4) become active. As shown in Ref. 8, at 37 °C, P_1 shows maximal level of activity compared to P_3 and is on within < 10 minutes of induction. The amount of transcripts generated from P_3 is very low and have been reported to be hardly detectable.[8] The P_4 promoter shows same level of activity as P_1 but produces antisense RNA. Although activity of P_4 promoter and its product, the antisense-RNA, is known, the target of the antisense RNA is not known till date. In passing it is important to mention that multi-promoter activity in the operon of TCS as observed in *B. pertussis*, has also been observed in other human pathogens.[9]

To model functioning of the *bvg* locus we consider only the activity of two promoters P_1 and P_2 in our model, as reasonable amount of experimental data is available in the literature for these two promoters.[8] Based on the activity of P_1 and P_2 promoters we consider two forms for each of the promoters, the inactive (P_{1i} and P_{2i}) and the active (P_{1a} and P_{2a}) forms. Transition from active to inactive state and vice versa is achieved through their interaction with TF (the phosphorylated dimer of the response regulator BvgA, A_{2P}),

$$P_{2a} + A_{2P} \underset{k_{u2}}{\overset{k_{b2}}{\rightleftharpoons}} P_{2i}, \tag{1}$$

$$P_{1i} + A_{2P} \underset{k_{u1}}{\overset{k_{b1}}{\rightleftharpoons}} P_{1a}. \tag{2}$$

In the above two equations repression of the constitutive promoter P_2 and activation of the induced promoter P_1 has been described in terms of the kinetics of interaction between TFs and promoters. To keep track of the transcripts generated due to P_1 and P_2, following Ref. 8, we consider two isoforms of mRNA generated from the *bvg* locus, m_{AS1} and m_{AS2}, respectively. At 25 °C, m_{AS2} is constitutively produced from the active state of P_2 promoter

$$P_{2a} \overset{k_{tp,20}}{\longrightarrow} m_{AS2}. \tag{3a}$$

After 2 hours of induction, level of m_{AS2} goes down but still maintains a low level of expression (see Fig. 3B of Ref. 8) which we assign to the residual activity of P_{2a}. After 20 minutes of induction, production of m_{AS2} remains still on, reaches a maxima, and then goes down which we attribute to the suppression of P_{2a} and the formation of P_{2i} altogether. At the onset of induction small amount TFs are produced, which increases the activity of the constitutive promoter rather than decreasing it. But around $\sim$20 minutes after induction pool of TFs cross a critical value and are sufficient to start repressing the constitutive promoter. Thus on a temporal scale, under inducing condition, synthesis of m_{AS2} gets controlled by both P_{2a} and P_{2i},

$$P_{2a} + P_{2i} \overset{k_{tp,21}}{\longrightarrow} m_{AS2}, \tag{3b}$$

which results into logistic kinetics of type $\sim x(1-x)$ when translated in terms of ordinary differential equation (ODE) (see Appendix). Unlike the transcripts generated due to P_2 activity, generation of m_{AS1} is solely governed by the the active form of P_1 promoter

$$P_{1a} \xrightarrow{k_{tp,11}} m_{AS1}. \tag{4}$$

Finally, we consider natural degradation of both the transcripts generated from P_1 and P_2,

$$m_{AS1} \xrightarrow{k_{d,m}} \varnothing, m_{AS2} \xrightarrow{k_{d,m}} \varnothing. \tag{5}$$

B. The two component system

Once transcribed from the locus, we consider translation of two isoforms m_{AS1} and m_{AS2} into dimers of sensor, BvgS (S_2), and response regulator, BvgA (A_2) proteins,

$$m_{AS1} \xrightarrow{k_{ss,1}} m_{AS1} + S_2, \tag{6a}$$

$$m_{AS2} \xrightarrow{k_{ss,2}} m_{AS2} + S_2, \tag{6b}$$

$$m_{AS1} \xrightarrow{k_{sa,1}} m_{AS1} + A_2, \tag{6c}$$

$$m_{AS2} \xrightarrow{k_{sa,2}} m_{AS2} + A_2. \tag{6d}$$

In reality the sensor and response regulator proteins are first translated as monomers and then dimerize.[3] Since dimers of BvgA, not the monomers, act as transcription factors for the activation of *bvg* locus, we have omitted kinetics of monomer formation and subsequent dimerization in our model and work instead with S_2 and A_2. As we show in the following, this simplification does not affect our analysis and modeling of the signal transduction network.

In bacterial TCS, autophosphorylation occurs at histidine residue of the sensor kinase, that serves as source of phosphate group and transfers the same to the aspartate residue of response regulator, acting as sink.[10–13] This orthodox two-step His-Asp phosphotransfer gets complicated in *B. pertussis* where signal transduction takes place via a unorthodox four-step His-Asp-His-Asp phosphotransfer mechanism,[14] where the first three steps (His-Asp-His) take place within the sensor protein BvgS and in the last step (His-Asp) phosphate group flows from the transmembrane sensor BvgS to the cytoplasmic response regulator BvgA. Although mathematical modeling of two-step phosphorelay has been reported in different context of bacterial signal transduction[15–19] very few studies have been undertaken to model the four-step phosphorelay kinetics.[20] In the present study we have adopted a simplified approach of what proposed by Kim and Cho.[20] Instead of detailed three-step (His-Asp-His) phosphotransfer mechanism within BvgS we consider autophosphorylation at S_2, the dimer of BvgS,

$$S_2 \underset{k_{dp,s2}}{\overset{k_{p,s2}}{\rightleftharpoons}} S_{2P}. \tag{7}$$

At this point it is important to mention that exact mechanism for the activation of BvgS in *B. pertussis* under temperature induction is not clear from the literature. To incorporate sensing of the external stimulus and subsequent activation of the TCS we have adopted the mechanism given in Eq. (7). Once phosphorylated the sensor protein transfers the phosphate group to their cognate response regulator A_2, the dimer of BvgA, mimicking the last step (His-Asp) of the four-step phosphotransfer mechanism. To model the phosphotransfer we have adopted the mechanism proposed by Batchelor and Goulian[16]

$$S_{2P} + A_2 \underset{k_{t,b}}{\overset{k_{t,f}}{\rightleftharpoons}} S_{2P} \cdot A_2 \xrightarrow{k_{t,a2}} S_2 + A_{2P}, \tag{8}$$

where $S_{2P} \cdot A_2$ is the Michaelis complex formed by S_{2P} and A_2. In addition to their kinase activity the sensor protein also exhibits phosphatase activity by removing the phosphate group from their cognate partner[12,16] thus showing bifunctional behavior

$$S_2 + A_{2P} \underset{k_{p,b}}{\overset{k_{p,f}}{\rightleftharpoons}} S_2 \cdot A_{2P} \xrightarrow{k_{p,a2}} S_2 + A_2. \tag{9}$$

Likewise the mRNA transcribed from the *bvg* locus, we consider natural degradation of different forms of sensor and response regulator proteins

$$S_2 \xrightarrow{k_{d,p}} \varnothing, S_{2P} \xrightarrow{k_{d,p}} \varnothing, A_2 \xrightarrow{k_{d,p}} \varnothing, A_{2P} \xrightarrow{k_{d,p}} \varnothing. \tag{10}$$

The phosphorylated dimer of the response regulator then exerts a positive feedback in the *bvg* locus thus activating and/or inhibiting the promoters of the locus (see Eqs. (1-2)). In addition they control the expression and/or repression of several downstream genes.

C. Differential gene regulation

To model regulation of downstream genes under induced condition we use the following TF binding properties of different promoters of downstream genes. The promoters for class 1 gene contain low affinity BvgA binding site far upstream of the transcriptional start site (TSP), as a result high level of A_{2P} is necessary to activate these genes and they are expressed quite late compared to class 2 and class 3 genes. Class 2 promoters contain high affinity BvgA binding site close to TSP and fairly low level of A_{2P} is sufficient to activate these genes. As a result, expression of class 2 genes becomes visible within very short period after induction. Class 3 gene, *bipA*, contains high affinity as well as low affinity BvgA binding site just upstream and downstream of TSP, respectively. Once induced, *bipA* becomes active almost at the same time like *fhaB* (class 2 gene) with the help of low amount of A_{2P}. At a critical concentration of BvgA gene expression becomes maximum and then it starts falling due to BvgA binding to the downstream low affinity binding site. The *frlAB* promoter (class 4) has been found to

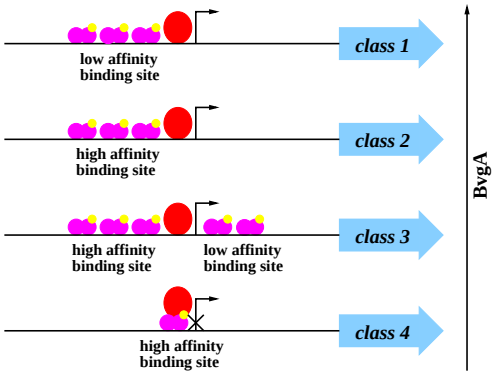

FIG. 2. (color online) Schematic diagram for differential gene regulation in *Bordetella pertussis*. The red blob is for RNA polymerase and the magenta dimers with yellow circle on top are for phosphorylated dimers of BvgA.

contain distinguishable BvgA binding site that overlaps with TSP.[21] Thus a very low level of BvgA may be able to suppress class 4 genes.

In Fig. 2 we schematically show regulation of four classes of genes as BvgA level increases. The binding kinetics of phosphorylated dimer of BvgA (A_{2P}) to the promoters of these four classes of genes are given in the Appendix (see Eqs. A1a-A4). While active, four classes of genes starts transcribing their corresponding mRNA

$$P_{clj,a} \xrightarrow{k_{tp,clj}} m_{clj}, \tag{11}$$

where $j = 1-4$. Likewise the transcripts generated from the *bvg* locus, we consider natural degradation of the four different classes of transcripts

$$m_{clj} \xrightarrow{k_{d,m}} \varnothing. \tag{12}$$

Before proceeding further we would like to mention that all the relevant symbols designating biochemical species used in this section are listed in the Table I.

III. RESULTS AND DISCUSSION

To check the validity of our proposed model, the kinetic network developed in the previous section has been translated into sets of coupled nonlinear ODEs. To understand functionality of temperature induced switch operative in the proposed model we first analyze the kinetics for *bvg* locus and the TCS using quasi-steady state approximation.[16] The full network kinetics is then numerically integrated for large set of parameters of the proposed model and compared with *in vivo* experimental results of Ref. 8.

A. Steady state analysis

According to the model described in the previous section total amount of sensor and response regulator proteins can be expressed by the conservation relation

$$[S_T] = [S_2] + [S_{2P}] + [S_{2P} \cdot A_2] + [S_2 \cdot A_{2P}], \tag{13}$$
$$[A_T] = [A_2] + [A_{2P}] + [S_{2P} \cdot A_2] + [S_2 \cdot A_{2P}], \tag{14}$$

where $[A_T]/[S_T] \approx k_{sa,2}/k_{ss,2} \approx 17$ (see Table II). Thus one can express essential features of the dynamics in terms of the response regulator protein. To realize the nature of amplification in gene expression at 37 °C and to analyze the steady state dynamics we divide the TCS signaling network into two modules, the autoregulation module and the phosphorylation (or post-translational) module.[16]

TABLE I. List of symbols (with initial values) used in the model

Symbol	Initial Value	Description
P_{1a}	0 nM	Active state of promoter P_1
P_{1i}	0.98 nM	Inactive state of promoter P_1
P_{2a}	0.98 nM	Active state of promoter P_2
P_{2i}	0 nM	Inactive state of promoter P_2
m_{AS1}	0 nM	Transcripts generated from P_{1a}
m_{AS2}	1.11 nM	Transcripts generated from P_{2a}
S_2	10.74 nM	Dimer of sensor BvgS
A_2	11.23 nM	Dimer of response regulator BvgA
S_{2P}	0 nM	Phosphorylated dimer of sensor BvgS
A_{2P}	0 nM	Phosphorylated dimer of response regulator BvgA (transcription factor)
$S_{2P} \cdot A_2$	0 nM	Michaelis constant formed by S_{2P} and A_2
$S_2 \cdot A_{2P}$	0 nM	Michaelis constant formed by S_2 and A_{2P}
$P_{cl1,a}$	0 nM	Active state of promoter for class 1 gene
$P_{cl1,i}$	0.98 nM	Inactive state of promoter for class 1 gene
$P_{cl2,a}$	0 nM	Active state of promoter for class 2 gene
$P_{cl2,i}$	0.98 nM	Inactive state of promoter for class 2 gene
$P_{cl3,a}$	0 nM	Active state of promoter for class 3 gene
$P_{cl3,i}$	0.98 nM	Inactive state of promoter for class 3 gene
$P_{cl4,a}$	0.98 nM	Active state of promoter for class 4 gene
$P_{cl4,i}$	0 nM	Inactive state of promoter for class 4 gene
m_{cl1}	0 nM	Transcripts generated from $P_{cl1,a}$
m_{cl2}	0 nM	Transcripts generated from $P_{cl2,a}$
m_{cl3}	0 nM	Transcripts generated from $P_{cl3,a}$
m_{cl4}	2.93 nM	Transcripts generated from $P_{cl4,a}$

1. Autoregulation module

In the limit $[A_T] > [S_T]$, $[A_T] \approx [A_2] + [A_{2P}]$ is a reasonable approximation as the Michaelis complexes $[S_{2P} \cdot A_2]$ and $[S_2 \cdot A_{2P}]$ show transient dynamics under this condition. Hence, the time evolution of $[A_T]$ can be written as

$$\frac{d[A_T]}{dt} \approx \frac{d[A_2]}{dt} + \frac{d[A_{2P}]}{dt},$$

in which using the explicit expressions for the terms in the right hand side (see Appendix) one arrives at

$$\frac{d[A_T]}{dt} \approx \tilde{\beta}_1(1 - F_2(A_P)) + \tilde{\beta}_2(1 - F_2(A_P))F_2(A_P) + \tilde{\beta}_3 F_1(A_P) - k_{d,p}[A_T]. \tag{15}$$

At steady state, equation (15) leads to

$$[A_T] \approx \beta_1(1 - F_2(A_P)) + \beta_2(1 - F_2(A_P))F_2(A_P) + \beta_3 F_1(A_P), \tag{16}$$

where $\beta_i = \tilde{\beta}_i/k_{d,p}$ $(i = 1, 2, 3)$. The first two terms on the right hand side of Eq. (16) arise due to P_2 promoter activity whereas the third term is solely due to P_1 promoter under inducing condition. In the limit of zero phosphorylation ($k_{p,s2} = 0$), i.e., at 25 °C, Eq. (16) leads to $[A_T] = \beta_1$ $(= k_{sa,2}k_{tp,20}/k_{d,m}k_{d,p})$. Thus, under zero stimulus system dynamics is solely governed by basal transcription ($k_{tp,20}$) and translation ($k_{sa,2}$) processes.

2. Phosphorylation module

Considering only the phosphotransfer kinetics (see Eqs. 7-9) and using the relations given in D.3 (see Appendix) we have at steady state

$$k_{p,s2}[S_2] = k_{dp,s2}[S_{2P}] - \frac{k_{t,a2}}{K_{Mt}}[S_{2P}][A_2], \qquad (17)$$

$$\frac{k_{p,a2}}{K_{Mp}}[S_2][A_{2P}] = \frac{k_{t,a2}}{K_{Mt}}[S_{2P}][A_2]. \qquad (18)$$

While deriving the above two expressions we have again considered the transient concentrations for the two Michaelis intermediates $[S_{2P} \cdot A_2]$ and $[S_2 \cdot A_{2P}]$ under the condition $[A_T] > [S_T]$ mentioned in the foregoing subsection. After some algebra Eqs. (17-18) provide

$$\frac{C_p}{A_{2P}} = \frac{C_t}{A_2} + 1, \qquad (19)$$

where $C_p = k_{p,s2}K_{Mp}/k_{p,a2}$ and $C_t = k_{dp,s2}K_{Mt}/k_{t,a2}$. Now, for $[A_T] \approx [A_2] + [A_{2P}]$, Eq. (19) gets transformed into

$$[A_{2P}] \approx \frac{1}{2}\left(C_t + C_p + [A_T]\right) - \frac{1}{2}\sqrt{\left(C_t + C_p + [A_T]\right)^2 - 4C_p[A_T]}, \qquad (20)$$

which is valid for $[A_{2P}] \leqslant [A_T]$.

In Fig. 3 we show steady state output of normalized $[A_{2P}]$ as a function of normalized $[A_T]$ for low and high temperature (red curves). In the model, temperature shift is done by tuning the control parameter $k_{p,s2}$. Sequential increase of temperature effectively makes a large pool of response regulator BvgA[22] which are ready to be phosphorylated as the autophosphorylation rate ($k_{p,s2}$) of the sensor protein is increased in the model, which in turn increases the pool of TFs, A_{2P}. The resulting curves show sigmoidal nature and saturate at high $[A_T]$ value. For zero auto dephosphorylation ($k_{dp,s2} = 0$) $C_t = 0$; in this case for $[A_T] > C_p$, Eq. (20) yields $[A_{2P}] \approx C_p$. Since C_p is a function of $k_{p,s2}$, for fixed set of other parameters of the model, a change in $k_{p,s2}$ brings in a change in the value of $[A_{2P}]$ (red curves). At this point it is pertinent to mention that in our model steady state output of $[A_{2P}]$ depends on both $[A_T]$ and the source of autophosphorylation, $k_{p,s2}$. In other words, the network output is sensitive when small fraction of response regulator is phosphorylated, $[A_{2P}] \leqslant [A_T]$, and is dependent on the source of phosphorylation. The intersections of the curve (blue) due to autoregulation module and the curves (red) due to phosphorylation module give a measure of the amplification in steady state output of $[A_{2P}]$ when temperature of the surrounding is increased. For a reasonable temperature shift, a small change in the $[A_T]$ value brings in a large jump in the $[A_{2P}]$ value, a signature of enhanced positive feedback controlled signal transduction.

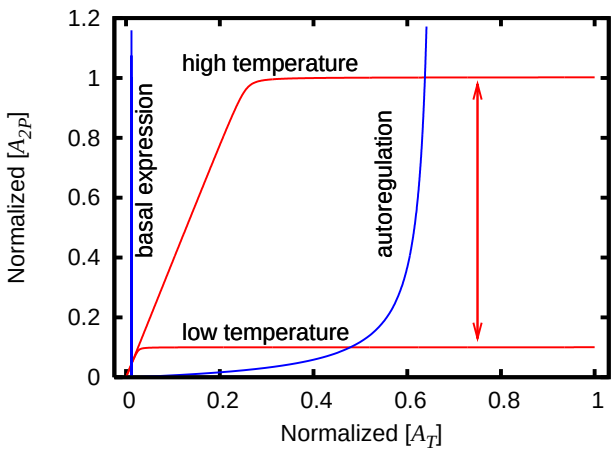

FIG. 3. (color online) The steady state behavior of the TCS circuit in terms of normalized $[A_{2P}]$ as a function of normalized $[A_T]$. The red curves are for phosphorylation module, Eq.(20), at low and high temperature. The blue switch like curve is due to autoregulation module, Eq.(16). While going from low to high temperature, a small change in the $[A_T]$ value makes a large amplification (the red double headed arrow) in the $[A_{2P}]$ value. The leftmost vertical blue line is for basal expression.

B. Time dependent dynamics

To study the time dependent behavior of different quantities of the model, the sets of nonlinear ODEs are solved by XPP (http://www.math.pitt.edu/∼bard/xpp/xpp.html) using the parameter set given in Table II. The consensus set of parameters used for numerical integration of the nonlinear ODEs are obtained using Parameter Estimation Toolkit (PET) (http://mpf.biol.vt.edu/pet/).

1. The *bvg* operon

In Fig. 4 we compare the numerically integrated data with experimental results,[8] for time evolution of transcripts m_{AS1} and m_{AS2} generated by the two promoters P_1 and P_2, respectively. While plotting the data we have scaled each transcripts value by the maximum of m_{AST} $(= m_{AS1} + m_{AS1})$ to compare simulated data with experimental results in a relative scale of 100. From Fig. 4 it is

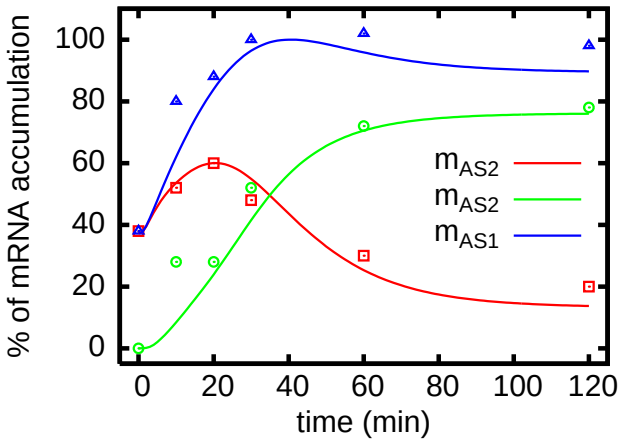

FIG. 4. (color online) Time evolution of transcripts m_{AS1} and m_{AS2} due to P_1 and P_2 activity, respectively. The open symbols are taken from Ref. 8 and the solid lines are results of numerical integration.

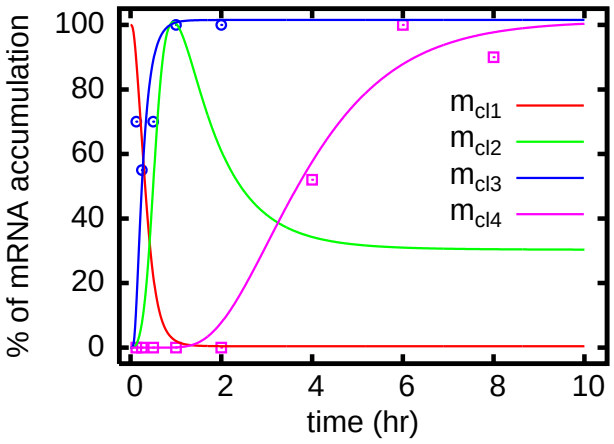

FIG. 6. (color online) Time evolution of four different classes of mRNA due to differential gene regulation. The open symbols are taken from Ref. 8 and the solid lines are due to numerical integration.

evident that our model captures the qualitative aspects of *in vivo* experimental results. To get an idea of how well our model can mimic the real system we define the amplification factor, f (= induced/basal) for mRNA expression which for experiment and simulation are $f_{exp} \approx 2.63$ and $f_{sim} = k_{tp,11}/k_{tp,20} \approx 2.28$, respectively, and are in good agreement.

2. The proteins

As the *bvg* operon gets switched on at higher temperature (37 °C) it starts producing a large pool of response regulator BvgA which is about $\geqslant 50$ fold higher than that what is produced at the non-inducing condition.[7,8,22] Experimental results show low level synthesis of sensor (BvgS) and response regulator (BvgA) proteins at low temperature (25 °C), but 6 hours after induction their level becomes 56 and 4 fold higher, respectively. In the next 18 hours level of BvgA protein goes down to 40 fold whereas level of BvgS protein finally increases to 17 fold.[8] In Fig. 5 we show qualitative agreement of simulated result with that of experimental data for fold increase of total BvgS (S_T) and total BvgA (A_T) protein. While caculating S_T and A_T we have used conservation relations (see Eqs. 13-14). It is interesting to note that although time evolution of protein levels show modulation, the relevant dynamics for the activation of the downstream genes takes place within first 8 hours of induction (see discussion in the following subsection).

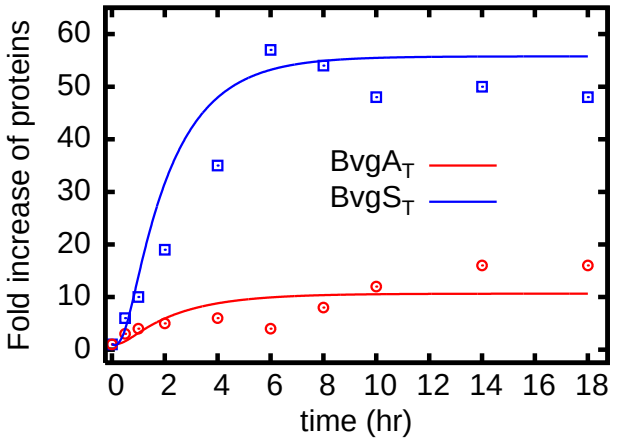

FIG. 5. (color online) Fold increase of total amount of sensor (S_T) and response regulator (A_T) protein. The dynamics is shown for first 18 hours after induction. The open symbols are taken from Ref. 8 and the solid lines are results of numerical integration.

3. Differential gene regulation

After 2 hours of induction total BvgA level increases only by ∼18 fold, but such low level of response regulator protein is enough to activate class 2 genes that encode the proteins for adherence due to high affinity binding site upstream of TSP. As a result, within 2 hours of induction the promoter for class 2 gene gets activated and the corresponding mRNA (m_{cl2}) level reaches its maximum value (see Fig. 6). After this 2 hours time window, level of BvgA rises and the accumulated amount is enough to bind the low affinity binding site of class 1 genes and to activate them. Thus, in a period of 2-6 hours of activation, class 1 genes gets fully *on* leading the corresponding mRNA (m_{cl1}) level to its maximum value (see Fig. 6).

Together with class 1 and class 2 genes we have shown the time evolution of class 3 and class 4 genes in Fig. 6. As mentioned in the introduction, although class 3 gene expression has not been observed in *B. pertussis* under

TABLE II. List of kinetic parameters (with values) used in the model

Parameter	Value	Description
k_{b1}	1.024×10^{-4} nM^{-1} s^{-1}	Association rate of A_{2P} and P_{1i}
k_{u1}	1.167×10^{-3} s^{-1}	Dissociation rate of A_{2P} from P_{1a}
k_{b2}	3.242×10^{-3} nM^{-1} s^{-1}	Association rate of A_{2P} and P_{2a}
k_{u2}	5.0×10^{-2} s^{-1}	Dissociation rate of A_{2P} from P_{2i}
$k_{tp,20}$	1.9×10^{-3} s^{-1}	Basal transcription rate from P_2 promoter
$k_{tp,21}$	9.386×10^{-3} nM^{-1} s^{-1}	Induced transcription rate from P_2 promoter
$k_{tp,11}$	4.083×10^{-3} s^{-1}	Induced transcription rate from P_1 promoter
$k_{d,m}$	1.667×10^{-3} s^{-1}	Degradation rate of mRNA
$k_{ss,1}$	6.667×10^{-3} s^{-1}	Synthesis rate of S_2 from m_{AS1}
$k_{ss,2}$	1.667×10^{-3} s^{-1}	Synthesis rate of S_2 from m_{AS2}
$k_{sa,1}$	4.167×10^{-2} s^{-1}	Synthesis rate of A_2 from m_{AS1}
$k_{sa,2}$	1.667×10^{-3} s^{-1}	Synthesis rate of A_2 from m_{AS2}
$k_{p,s2}$	8.333×10^{-3} s^{-1}	Phosphorylation rate of S_2
$k_{dp,s2}$	3.333×10^{-3} s^{-1}	Dephosphorylation rate of S_{2P}
$k_{t,f}$	8.532×10^{-3} nM^{-1} s^{-1}	Association rate of S_{2P} and A_2
$k_{t,b}$	1.667×10^{-3} s^{-1}	Dissociation rate of $S_{2P} \cdot A_2$
$k_{t,a2}$	8.333×10^{-2} s^{-1}	Phosphate transfer rate from S_{2P} to A_2
$k_{p,f}$	3.413×10^{-5} nM^{-1} s^{-1}	Association rate of S_2 and A_{2P}
$k_{p,b}$	1.333×10^{-3} s^{-1}	Dissociation rate of $S_2 \cdot A_{2P}$
$k_{p,a2}$	5.0×10^{-2} s^{-1}	Phosphate removal rate from A_{2P} by S_2
$k_{d,p}$	1.667×10^{-4} s^{-1}	Degradation rate of protein
$k_{b,11}$	8.533×10^{-7} nM^{-1} s^{-1}	Association rate of A_{2P} and $P_{cl1,i}$
$k_{u,11}$	1.667×10^{-6} s^{-1}	Dissociation rate of A_{2P} from $P_{cl1,i1}$
$k_{b,12}$	1.365×10^{-6} nM^{-1} s^{-1}	Association rate of A_{2P} and $P_{cl1,i1}$
$k_{u,12}$	3.333×10^{-6} s^{-1}	Dissociation rate of A_{2P} from $P_{cl1,i2}$
$k_{b,13}$	1.706×10^{-6} nM^{-1} s^{-1}	Association rate of A_{2P} and $P_{cl1,i2}$
$k_{u,13}$	8.333×10^{-6} s^{-1}	Dissociation rate of A_{2P} from $P_{cl1,a}$
$k_{b,21}$	5.119×10^{-4} nM^{-1} s^{-1}	Association rate of A_{2P} and $P_{cl2,i}$
$k_{u,21}$	1.667×10^{-4} s^{-1}	Dissociation rate of A_{2P} from $P_{cl2,i1}$
$k_{b,22}$	1.706×10^{-3} nM^{-1} s^{-1}	Association rate of A_{2P} and $P_{cl2,i1}$
$k_{u,22}$	3.333×10^{-4} s^{-1}	Dissociation rate of A_{2P} from $P_{cl2,i2}$
$k_{b,23}$	1.706×10^{-3} nM^{-1} s^{-1}	Association rate of A_{2P} and $P_{cl2,i2}$
$k_{u,23}$	5.0×10^{-4} s^{-1}	Dissociation rate of A_{2P} from $P_{cl2,a}$
$k_{b,31}$	8.533×10^{-5} nM^{-1} s^{-1}	Association rate of A_{2P} and $P_{cl3,i}$
$k_{u,31}$	1.667×10^{-4} s^{-1}	Dissociation rate of A_{2P} from $P_{cl3,i1}$
$k_{b,32}$	1.365×10^{-4} nM^{-1} s^{-1}	Association rate of A_{2P} and $P_{cl3,i1}$
$k_{u,32}$	3.333×10^{-4} s^{-1}	Dissociation rate of A_{2P} from $P_{cl3,a}$
$k_{b,33}$	1.706×10^{-6} nM^{-1} s^{-1}	Association rate of A_{2P} and $P_{cl3,a}$
$k_{u,33}$	5.0×10^{-4} s^{-1}	Dissociation rate of A_{2P} from $P_{cl3,i2}$
$k_{b,34}$	3.413×10^{-6} nM^{-1} s^{-1}	Association rate of A_{2P} and $P_{cl3,i2}$
$k_{u,34}$	6.667×10^{-4} s^{-1}	Dissociation rate of A_{2P} from $P_{cl3,i3}$
$k_{b,35}$	4.266×10^{-6} nM^{-1} s^{-1}	Association rate of A_{2P} and $P_{cl3,i3}$
$k_{u,35}$	8.333×10^{-4} s^{-1}	Dissociation rate of A_{2P} from $P_{cl3,i4}$
$k_{b,41}$	1.706×10^{-4} nM^{-1} s^{-1}	Association rate of A_{2P} and $P_{cl4,a}$
$k_{u,41}$	1.667×10^{-4} s^{-1}	Dissociation rate of A_{2P} from $P_{cl4,i}$
$k_{tp,cl1}$	5.167×10^{-3} s^{-1}	Transcription rate from $P_{cl1,a}$ promoter
$k_{tp,cl2}$	5.083×10^{-3} s^{-1}	Transcription rate from $P_{cl2,a}$ promoter
$k_{tp,cl3}$	6.083×10^{-3} s^{-1}	Transcription rate from $P_{cl3,a}$ promoter
$k_{tp,cl4}$	5.0×10^{-3} s^{-1}	Transcription rate from $P_{cl4,a}$ promoter

temperature induction, we predict that proper modulation of external temperature may lead to expression of class 3 gene in *B. pertussis* as gradual tuning of external temperature slowly accumulates the transcription factor in a graded response manner.[22] Similarly, expression of class 4 gene can be achieved by incorporating a plasmid containing *frlAB* fused with *lacZ* from *B. bronchiseptica* into *B. pertussis*. Similar kind of technique has been used to express *ptx* promoter from *B. pertussis* in *B. bronchiseptica*.[23]

IV. CONCLUSION AND OUTLOOK

To conclude, we have developed a mathematical model to study signal transduction and differential gene regulation in *B. pertussis* under the influence of temperature elevation. The proposed model takes care of possible elementary kinetics of the biochemical interactions between several system components. To understand the molecular switch operative in the BvgAS TCS, a quasi steady state analysis has been performed which reveals temperature induced molecular switch that responds to the external stimulus in a graded manner. The very nature of the graded response has been shown as the consequence of positive feedback motif present within the *bvgAS* operon.

Outcome of the graded response gets reflected in the large accumulation of the TF, which then controls the expression of several downstream genes including the genes for adherence and toxin. The later features have been observed via numerical integration of the coupled nonlinear ODEs for large set of parameters. The resultant numerical results essentially capture the qualitative features of the network dynamics performed *in vivo*. On the basis of our developed model we have made novel testable prediction for the temperature induced class 3 gene expression. To the best of our knowledge, the model we propose here is the first theoretical venture to understand properties of complex signal transduction network present in *B. pertussis*.

We hope that our *in silico* study will inspire more experiments in the coming days to address subtle issues of the network that are yet to be explored. One of such issues is the characterization of exact target and functioning of the antisense RNA, transcribed from P_4 promoter of *bvgAS* operon. In addition, one may find it interesting to make quantitative measurement of different proteins generated due to activity of the four classes of downstream genes. Information from these new experimental findings will certainly help one to build a more realistic model in future.

ACKNOWLEDGMENTS

We express our sincerest gratitude to Indrani Bose and Sudip Chattopadhyay for stimulating discussions. AB acknowledges Council of Scientific and Industrial Research (CSIR), Government of India, for a research fellowship (09/015(0375)/2009-EMR-I). SKB acknowledges support from Bose Institute through an initial start up fund.

Appendix A: Promoter kinetics of downstream genes

The active and inactive forms of four different promoters of the downstream genes are modeled as $P_{clj,a}$ and $P_{clj,i}$ $(j = 1, 2, 3, 4)$, respectively. Considering cooperativity in binding of TFs (A_{2P}) to the high/low affinity binding site of these promoters we model binding kinetics as follows,

For class 1 gene:

$$P_{cl1,i} + A_{2P} \underset{k_{u,11}}{\overset{k_{b,11}}{\rightleftharpoons}} P_{cl1,i1}, \tag{A1a}$$

$$P_{cl1,i1} + A_{2P} \underset{k_{u,12}}{\overset{k_{b,12}}{\rightleftharpoons}} P_{cl1,i2}, \tag{A1b}$$

$$P_{cl1,i2} + A_{2P} \underset{k_{u,13}}{\overset{k_{b,13}}{\rightleftharpoons}} P_{cl1,a}. \tag{A1c}$$

For class 2 gene:

$$P_{cl2,i} + A_{2P} \underset{k_{u,21}}{\overset{k_{b,21}}{\rightleftharpoons}} P_{cl2,i1}, \tag{A2a}$$

$$P_{cl2,i1} + A_{2P} \underset{k_{u,22}}{\overset{k_{b,22}}{\rightleftharpoons}} P_{cl2,i2}, \tag{A2b}$$

$$P_{cl2,i2} + A_{2P} \underset{k_{u,23}}{\overset{k_{b,23}}{\rightleftharpoons}} P_{cl2,a}. \tag{A2c}$$

For class 3 gene:

$$P_{cl3,i} + A_{2P} \underset{k_{u,31}}{\overset{k_{b,31}}{\rightleftharpoons}} P_{cl3,i1}, \tag{A3a}$$

$$P_{cl3,i1} + A_{2P} \underset{k_{u,32}}{\overset{k_{b,32}}{\rightleftharpoons}} P_{cl3,a}, \tag{A3b}$$

$$P_{cl3,a} + A_{2P} \underset{k_{u,33}}{\overset{k_{b,33}}{\rightleftharpoons}} P_{cl3,i2}, \tag{A3c}$$

$$P_{cl3,i2} + A_{2P} \underset{k_{u,34}}{\overset{k_{b,34}}{\rightleftharpoons}} P_{cl3,i3}, \tag{A3d}$$

$$P_{cl3,i3} + A_{2P} \underset{k_{u,35}}{\overset{k_{b,35}}{\rightleftharpoons}} P_{cl3,i4}. \tag{A3e}$$

For class 4 gene:

$$P_{cl4,a} + A_{2P} \underset{k_{u,41}}{\overset{k_{b,41}}{\rightleftharpoons}} P_{cl4,i}, \tag{A4}$$

In the above set of equations $P_{clj,ik}$ $(k = 1, 2, \ldots)$ represents the inactive intermediate states of the different classes of promoters.

Appendix B: Promoter kinetics of bvg locus

As mentioned in the main text we consider a single copy of the *bvg* gene, with conservation relations $[P_{2i}] + [P_{2a}] = 1$ and $[P_{1i}] + [P_{1a}] = 1$ for the two promoters controlling functionality of the *bvgAS* operon. Dynamical equations for the promoter kinetics thus can be written as

$$\frac{d[P_{2a}]}{dt} = -k_{b2}[P_{2a}][A_{2P}] + k_{u2}[P_{2i}], \tag{B1}$$

$$\frac{d[P_{1a}]}{dt} = k_{b1}[P_{1i}][A_{2P}] - k_{u1}[P_{1a}], \tag{B2}$$

which at the steady state ($d[P_{2a}]/dt = d[P_{1a}]/dt = 0$) give,

$$\begin{aligned} &[P_{1a}] = F_1(A_{2P}), [P_{1i}] = 1 - F_1(A_{2P}), \\ &[P_{2a}] = 1 - F_2(A_{2P}), [P_{2i}] = F_2(A_{2P}), \end{aligned} \tag{B3}$$

where

$$F_1(A_{2P}) = \frac{[A_{2P}]_1}{1 + [A_{2P}]_1}, F_2(A_{2P}) = \frac{[A_{2P}]_2}{1 + [A_{2P}]_2},$$

with $[A_{2P}]_i = [A_{2P}]/K_i$ for $K_i = k_{ui}/k_{bi}$ $(i = 1, 2)$.

Appendix C: mRNA kinetics

Time evolution of the transcripts generated from the two promoters P_2 and P_1 are given by the following set of equations, respectively,

$$\frac{d[m_{AS2}]}{dt} = k_{tp,20}[P_{2a}] + k_{tp,21}[P_{2a}][P_{2i}] - k_{d,m}[m_{AS2}], \quad \text{(C1)}$$

$$\frac{d[m_{AS1}]}{dt} = k_{tp,11}[P_{1a}] - k_{d,m}[m_{AS1}]. \quad \text{(C2)}$$

Along with the steady state expression for the two promoters given in equation (B3), one arrives at the following expressions for concentrations of the two transcripts at steady state ($d[m_{AS2}]/dt = d[m_{AS1}]/dt = 0$)

$$[m_{AS2}] = \frac{k_{tp,20}}{k_{d,m}}(1 - F_2(A_{2P})) + \frac{k_{tp,21}}{k_{d,m}}(1 - F_2(A_{2P}))F_2(A_{2P}),$$

$$[m_{AS1}] = \frac{k_{tp,11}}{k_{d,m}}F_1(A_{2P}). \quad \text{(C3)}$$

Appendix D: Phosphotransfer kinetics

From the kinetics of phosphate donation from sensor to response regulator (kinase), and phosphate withdrawal from response regulator by sensor (phosphatase), we have two dynamical equations for the two intermediates $S_{2P} \cdot A_2$ and $S_2 \cdot A_{2P}$

$$\frac{d[S_{2P} \cdot A_2]}{dt} = k_{t,f}[S_{2P}][A_2] - (k_{t,b} + k_{t,a2})[S_{2P} \cdot A_2], \quad \text{(D1)}$$

$$\frac{d[S_2 \cdot A_{2P}]}{dt} = k_{p,f}[S_2][A_{2P}] - (k_{p,b} + k_{p,a2})[S_2 \cdot A_{2P}]. \quad \text{(D2)}$$

While writing the above two equations we have neglected degradation of the intermediates as they show transient dynamics. Now by imposing quasi-steady state conditions on equations (D1-D2) we have

$$[S_{2P} \cdot A_2] = \frac{[S_{2P}][A_2]}{K_{Mt}}, [S_2 \cdot A_{2P}] = \frac{[S_2][A_{2P}]}{K_{Mp}}, \quad \text{(D3)}$$

where $K_{Mt} = (k_{t,b} + k_{t,a2})/k_{t,f}$ and $K_{Mp} = (k_{p,b} + k_{p,a2})/k_{p,f}$ are the Michaelis constants for the kinase and the phosphatase activity of the sensors, respectively.

Appendix E: Protein kinetics

The dynamical equations representing kinetics of the different forms of sensor and response regulator proteins can be represented by the following sets of ordinary differential equations

$$\frac{d[S_2]}{dt} = \tilde{\alpha}_1(1 - F_2(A_{2P})) + \tilde{\alpha}_2(1 - F_2(A_{2P}))F_2(A_{2P}) + \tilde{\alpha}_3F_1(A_{2P}) - k_{p,s2}[S_2] + k_{dp,s2}[S_{2P}] + \frac{k_{t,a2}}{K_{Mt}}[S_{2P}][A_2] - k_{d,p}[S_2], \quad \text{(E1)}$$

$$\frac{d[S_{2P}]}{dt} = k_{p,s2}[S_2] - k_{dp,s2}[S_{2P}] - \frac{k_{t,a2}}{K_{Mt}}[S_{2P}][A_2] - k_{d,p}[S_{2P}], \quad \text{(E2)}$$

$$\frac{d[A_2]}{dt} = \tilde{\beta}_1(1 - F_2(A_{2P})) + \tilde{\beta}_2(1 - F_2(A_{2P}))F_2(A_{2P}) + \tilde{\beta}_3F_1(A_{2P}) - \frac{k_{t,a2}}{K_{Mt}}[S_{2P}][A_2] + \frac{k_{p,a2}}{K_{Mp}}[S_2][A_{2P}] - k_{d,p}[A_2], \quad \text{(E3)}$$

$$\frac{d[A_{2P}]}{dt} = \frac{k_{t,a2}}{K_{Mt}}[S_{2P}][A_2] - \frac{k_{p,a2}}{K_{Mp}}[S_2][A_{2P}] - k_{d,p}[A_{2P}], \quad \text{(E4)}$$

where

$$\tilde{\alpha}_1 = k_{ss,2}\frac{k_{tp,20}}{k_{d,m}}, \tilde{\alpha}_2 = k_{ss,2}\frac{k_{tp,21}}{k_{d,m}}, \tilde{\alpha}_3 = k_{ss,1}\frac{k_{tp,11}}{k_{d,m}},$$

$$\tilde{\beta}_1 = k_{sa,2}\frac{k_{tp,20}}{k_{d,m}}, \tilde{\beta}_2 = k_{sa,2}\frac{k_{tp,21}}{k_{d,m}}, \tilde{\beta}_3 = k_{sa,1}\frac{k_{tp,11}}{k_{d,m}}.$$

While writing Eqs.(E1-E4) we have used the steady state expressions for $[m_{AS1}], [m_{AS2}], [S_{2P} \cdot A_2]$ and $[S_2 \cdot A_{2P}]$ given by Eqs.(C3) and (D3).

[1] U. Alon, *An Introduction to Systems Biology: Design Principles of Biological Circuits* (CRC Press, New York, 2007).
[2] A. Preston, J. Parkhill, and D. J. Maskell, Nat Rev Microbiol **2**, 379 (2004).
[3] D. Beier and R. Gross, Adv Exp Med Biol **631**, 149 (2008).
[4] P. A. Cotter and A. M. Jones, Trends Microbiol **11**, 367 (2003).
[5] P. Steffen, S. Goyard, and A. Ullmann, EMBO J **15**, 102 (1996).
[6] C. R. Roy, J. F. Miller, and S. Falkow, Proc Natl Acad Sci U S A **87**, 3763 (1990).
[7] V. Scarlato, A. Prugnola, B. Aricó, and R. Rappuoli, Proc Natl Acad Sci U S A **87**, 10067 (1990).
[8] V. Scarlato, B. Aricò, A. Prugnola, and R. Rappuoli, EMBO J **10**, 3971 (1991).
[9] V. Donà, S. Rodrigue, E. Dainese, G. Palù, L. Gaudreau, R. Manganelli, and R. Provvedi, J Bacteriol **190**, 5963 (2008).
[10] J. L. Appleby, J. S. Parkinson, and R. B. Bourret, Cell **86**, 845 (1996).
[11] J. A. Hoch, Curr Opin Microbiol **3**, 165 (2000).
[12] M. T. Laub and M. Goulian, Annu Rev Genet **41**, 121 (2007).
[13] A. M. Stock, V. L. Robinson, and P. N. Goudreau, Annu Rev Biochem **69**, 183 (2000).
[14] M. A. Uhl and J. F. Miller, EMBO J **15**, 1028 (1996).
[15] S. K. Banik, A. T. Fenley, and R. V. Kulkarni, Phys Biol **6**, 046008 (2009).
[16] E. Batchelor and M. Goulian, Proc Natl Acad Sci U S A **100**, 691 (2003).
[17] A. Kato, A. Y. Mitrophanov, and E. A. Groisman, Proc Natl Acad Sci U S A **104**, 12063 (2007).
[18] G. Shinar, R. Milo, M. R. Martínez, and U. Alon, Proc Natl Acad Sci U S A **104**, 19931 (2007).
[19] K. Sureka, B. Ghosh, A. Dasgupta, J. Basu, M. Kundu, and I. Bose, PLoS One **3**, e1771 (2008).
[20] J. R. Kim and K. H. Cho, Comput Biol Chem **30**, 438 (2006).

[21] B. J. Akerley, P. A. Cotter, and J. F. Miller, Cell **80**, 611 (1995).
[22] A. Prugnola, B. Aricò, R. Manetti, R. Rappuoli, and V. Scarlato, Microbiology **141**, 2529 (1995).
[23] C. L. Williams and P. A. Cotter, J Bacteriol **189**, 1974 (2007).